Multiorgan Visceral Hemangiomas Presenting with Sequential Ruptures and Hemorrhage, Cardiac Thrombus, and Thromboembolic Phenomenon

Subhash Kumar[1] Kamlesh Gunjan[2] Rajeev N. Priyadarshi[1] Mala Mahto[3]

[1] Department of Radiodiagnosis, All India Institute of Medical Sciences Patna, Patna, Bihar, India
[2] Department of Urology, All India Institute of Medical Sciences Patna, Patna, Bihar, India
[3] Department of Biochemistry, All India Institute of Medical Sciences Patna, Patna, Bihar, India

Address for correspondence Subhash Kumar, MBBS, MD, DM, Department of Radiodiagnosis, All India Institute of Medical Sciences Patna, Phulwarisharif, Patna, Bihar 801507, India (e-mail: drsubhash.dm@gmail.com).

J Gastrointestinal Abdominal Radiol ISGAR 2023;6:47–52.

Abstract

Vascular anomalies can be seen in a disseminated or diffuse state to involve multiple superficial and deep sites. Large and diffuse lesions are known to induce a hemorrhagic tendency. The authors present, which they believe is the first case of multiorgan hemangiomas with rupture at multiple sites, along with hitherto unreported cardiac thrombus, with arterial and venous thromboembolic events, ultimately ending with the patient's demise.

Keywords
- hemangioma
- thrombus
- thromboembolism
- embolization

Introduction

Deep-seated vascular anomalies (VAs) can present late in adulthood, especially if superficial lesions are not present.[1–5] Hepatic hemangiomas are seen in 0.7 to 7% of the population, while renal hemangiomas are extremely rare.[6–8] Hematologic complications, both thrombotic and hemorrhagic, seen especially with giant/diffuse lesions, can have extremely complex management.[8–10]

Case Report

A 24-year-old, previously healthy woman, was operated for sudden hemoperitoneum presumably due to ectopic pregnancy, but not found intraoperatively. She presented to us 1.5 months later with flank pain and hematuria, and was found to have a nonexcreting right kidney harboring a large hemangioma with perinephric hematoma, and multiple smaller lesions in other viscera (►**Figs. 1** and **2**). Thrombi were seen in left atrium, left common iliac artery, right femoral artery, and left femoral vein with tortuous vessels in the left lower lung lobe (►**Fig. 2**). A renal embolization was refused. Fresh-frozen plasma, whole blood, and tranexamic acid were given, following which the hemoglobin improved transiently, and fresh hematuria stopped after 5 days. A two-dimensional echocardiogram showed no valvular or functional pathology. Right nephrectomy was advised, but she redeveloped hematuria after 3 days, with significantly deranged blood parameters and D-dimer but normal fibrinogen levels (►**Table 1**). After 2 days, family agreed for embolization, however, at morning, she developed a left parieto-occipital hematoma with right hemiparesis and altered sensorium (►**Fig. 2**). Her

article published online
August 15, 2022

DOI https://doi.org/10.1055/s-0042-1751252.
ISSN 2581-9933.

Thieme Medical and Scientific Publishers Pvt. Ltd., A-12, 2nd Floor, Sector 2, Noida-201301 UP, India

Table 1 Salient essential investigations of the patients

Date	Liver function	Renal function	Coagulation	Hemogram
26/02/2021	TBil 4.17 mg/dL DBil 2.42 mg/dL ALT 32.3 U/L AST 73.6 U/L	Urea 28.7 mg/dL Creatinine 0.69 mg/dL	PT/INR 13.6 s/1.0	Hb 9.2 g/dL WBC 10.54×10^3/μLt Platelet 268×10^3/μLt
09/03/2021				Hb 7.9 g/dL WBC 11.79×10^3/μLt Platelet 327×10^3/μLt
19/03/2021			PT/INR 13.07 s/0.97 aPTT 20.6 s (26–40 s) Fibrinogen 254 mg/dL (100–400 mg/dL) Protein S Ag Free 55% (60–140) Protein C activity 03% (70–140) Antithrombin Act 129	
20/03/2021	TBil 7.20 mg/dL DBil 5.03 mg/dL ALT 22.2 U/L AST 48.0 U/L	Urea 33.3 mg/dL Creatinine 0.53 mg/dL		Hb 4.3 g/dL WBC 17.49×10^3/μLt Platelet 208×10^3/μLt
21/03/2021	TBil 5.06 mg/dL DBil 3.46 mg/dL ALT 20.5 U/L AST 53.5 U/L			Hb 6.7 g/dL WBC 18.03×10^3/μLt Platelet 210×10^3/μLt
22/03/2021			PT/INR 19.8 s/1.50	Hb 5.9 g/dL WBC 13.43×10^3/μLt Platelet 207×10^3/μLt
23/03/2021	TBil 4.48 mg/dL DBil 2.92 mg/dL ALT 75.8 U/L AST 268.8 U/L	Urea 35.0 mg/dL Creatinine 0.69 mg/dL	PT/INR 28.06 s/2.20	Hb 5.6 g/dL WBC 21.00×10^3/μLt Platelet 102×10^3/μLt
24/03/2021		Urea 64.9 mg/dL Creatinine 1.25 mg/dL	Plasma D-dimer 7.23 μg/mL (< 0.2 μg/mL)	Hb 7.3 g/dL WBC 22.90×10^3/μLt Platelet 140×10^3/μLt
25/03/2021	TBil 6.16 mg/dL DBil 3.68 mg/dL ALT 119.3 U/L AST 299.7 U/L	Urea 103.9 mg/dL Creatinine 2.20 mg/dL	PT/INR 14.72 s/1.10 aPTT 23.50 s (30–40 s)	Hb 4.0 g/dL WBC 23.09×10^3/μLt Platelet 140×10^3/μLt
26/03/2021	TBil 4.81 mg/dL DBil 3.10 mg/dL ALT 139.6 U/L AST 273.3 U/L	Urea 127.2 mg/dL Creatinine 2.79 mg/dL	PT/INR 13.12 s/0.97	Hb 3.7 g/dL WBC 25.77×10^3/μLt Platelet 120×10^3/μLt
27/03/2021	TBil 4.64 mg/dL DBil 3.01 mg/dL ALT 96.6 U/L AST 139.7 U/L	Urea 150.4 mg/dL Creatinine 3.54 mg/dL		Hb 5.8 g/dL WBC 21.75×10^3/μLt Platelet 78×10^3/μLt
28/03/2021	TBil 4.86 mg/dL DBil 3.02 mg/dL ALT 72.7 U/L AST 100.2 U/L	Urea 138.9 mg/dL Creatinine 2.89 mg/dL		Hb 5.8 g/dL WBC 30.17×10^3/μLt Platelet 150×10^3/μLt
29/03/2021	TBil 4.83 mg/dL DBil 3.13 mg/dL ALT 57.8 U/L AST 127.3 U/L	Urea 138.5 mg/dL Creatinine 3.24 mg/dL		Hb 5.6 g/dL WBC 30.03×10^3/μLt Platelet 124×10^3/μLt
30/03/2021	TBil 4.47 mg/dL DBil 2.89 mg/dL ALT 40.7 U/L AST 90.9 U/L	Urea 123 mg/dL Creatinine 337 mg/dL	PT/INR 13.39 s/0.99	Hb 6.6 g/dL WBC 34.19×10^3/μLt Platelet 53×10^3/μLt
Other investigation	CA 19–9 6.99 U/mL (< 37 U/mL) CEA 1.70 ng/mL (0–2.5 ng/mL) CA 125 18.8 U/mL (< 35 U/mL)			

Abbreviations: ALT, alanine aminotransferase; aPTT, activated partial thromboplastin time; AST, aspartate aminotransferase; CA, cancer antigen; CEA, carcinoembryonic antigen; DBil, direct bilirubin; Hb, hemoglobin; INR, international normalized ratio; Protein S Ag, protein S antigen; PT, prothrombin time; TBil, total-value bilirubin; WBC, white blood cell.

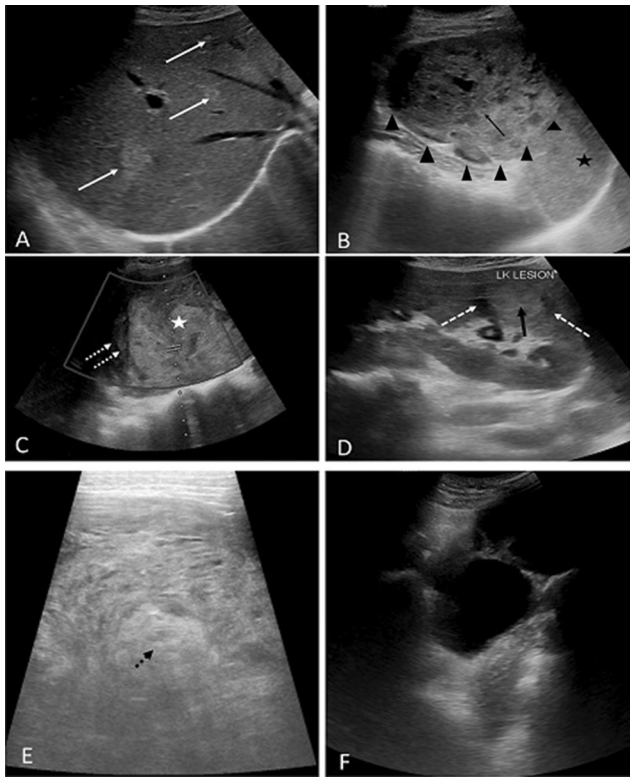

Fig. 1 Ultrasound panel showing images acquired immediately after admission. (**A**) Liver scan showing multiple well-defined hyperechoic lesion of variable sizes (solid white arrows). (**B**) Heterogeneous hypoechoic lesion (outlined by black arrowheads) with internal cystic spaces in the spleen (black solid arrow), the normal spleen is seen at the lower part (black star). (**C**) Right kidney shows a large predominantly hyperechoic lesion (white star) with a heterogeneous hypoechoic collection adjacent to it (dashed white arrows). (**D**) Left kidney shows a hyperechoic lesion (small black solid arrow) with a hypoechoic rim around it (dashed white arrows). (**E**) Abdomen scan showing a hyperechoic lesion (small dashed black arrow) within the omentum which is draped all around it. (**F**) Complex cystic space-occupying lesion in the pelvis.

international normalized ratio was raised, and a computed tomography angiography showed no vascular abnormality (►**Fig. 2**). Emergency right renal embolization was performed (►**Fig. 3**). Subsequently, decompressive craniectomy and hematoma evacuation was performed. During surgery, yellowish gray tumoral fragments were also extracted from the posterior edge of the hematoma. Histopathologic examination had shown vascular lesion with dilated cavernous spaces which were lined with endothelium, without any mature vascular architecture. She was reoperated the next day due to multifocal bihemispherical hemorrhages and large extradural hematoma, with sudden neurological deterioration (►**Fig. 2**).

She also had altered liver and renal profiles, and underwent dialysis. On the 5th day of surgery, she developed bleeding per-vaginam and rectum, and died on the 7th day. During this ordeal, she was infused with a total of 30 units of blood and 20 units of fresh-frozen plasma.

Discussion

Adult visceral hemangiomas are a common incidental finding, although renal lesions are rare, and can present with rupture and hematuria, requiring surgery/embolization.[6–8,11] Multiorgan ruptured hemangiomas, however, could not be found in the literature by the authors.

Our case has few peculiarities:

1. She had hemoperitoneum, however, ectopic pregnancy was not found intraoperatively, and points toward bowel/omental/peritoneal hemangioma.

2. Concomitant hemorrhages and thrombotic/embolic phenomenon were seen, complicating the management.

3. Multiorgan ruptured lesions were seen. The intracranial hemorrhage, however, could have been due to the ruptured lesions or the ongoing coagulopathy.

4. Cardiac thrombus in this setting is being reported for the first time, and we hypothesize it to be a manifestation of the coagulopathy. Venous thrombosis and embolism have known association with VAs, elevated D-dimer seen in up to 42% cases, and syndromic lesions, for example, Klippel–Trenaunay syndrome having even higher rates.[9] However, cardiac and arterial thrombosis or embolism have not been reported. The coagulopathy in such cases is multifactorial and trauma or surgery also predisposes to it.[10] Thus, a minimally invasive endovascular procedure is recommended.

The blue rubber bleb nevus syndrome (BRBNS) is a syndrome of multiple superficial and deep venous

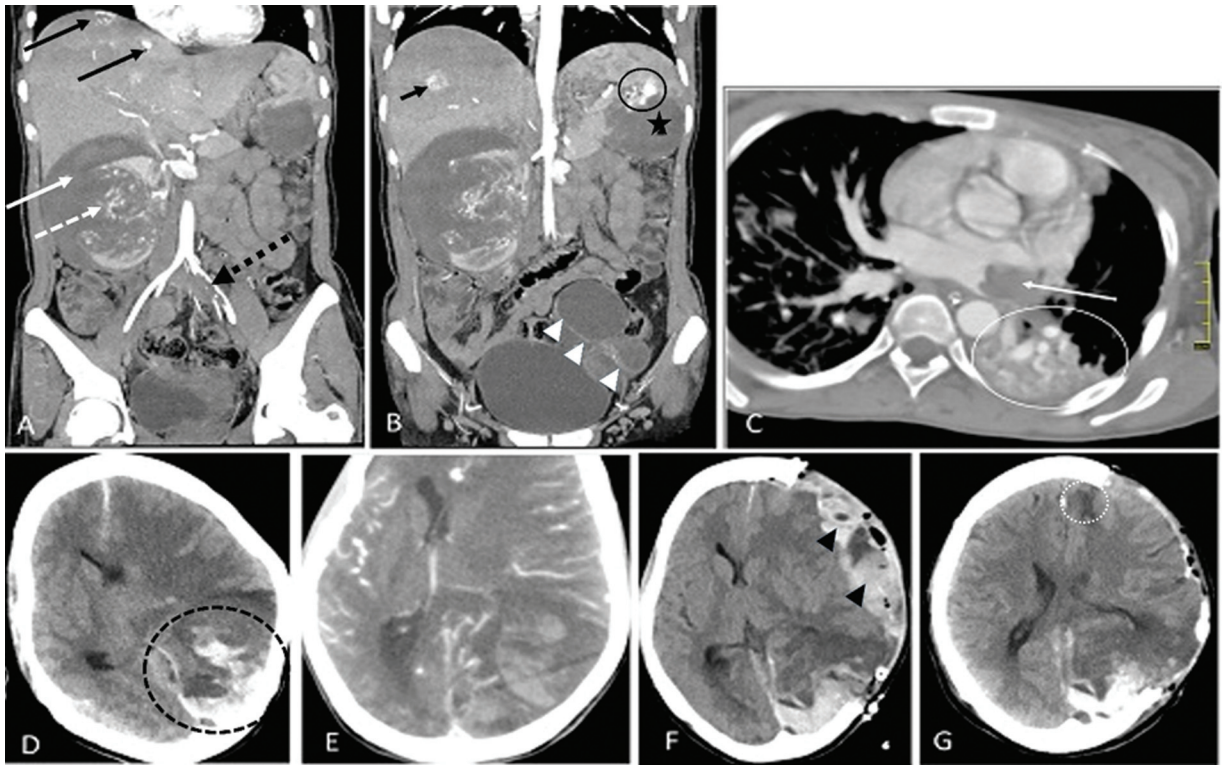

Fig. 2 Computed tomography (CT) panel. (**A**) Coronal image showing multiple nodular and peripherally enhancing lesions in liver (black arrows), and the right kidney is almost completely replaced by a heterogeneous nodular enhancing mass (dashed white arrow) with perinephric hematoma (solid white arrow), the lesion having been ruptured and the lateral margin of kidney not visualized, a filing defect is seen in the left common iliac artery due to thrombus (dashed black arrow). (**B**) Coronal image showing a peripherally enhancing liver lesion (short black arrow) and nodule enhancing lesion in spleen (black circle) with a hematoma (black star), white arrowhead points to a complex, predominantly cystic lesion in the pelvis. (**C**) Axial image of the chest showing a hypodense thrombus in the left atrium (white arrow) and a bunch of enlarged tortuous vessels within an area of consolidation in the superior segment of the left lower lobe (white oval). (**D**) Head CT on the day of renal embolization, showing left parieto-occipital lobe hematoma (dashed black circle) with mass effect and midline shift to the right. (**E**) Axial source image of a CT angiography of the head showing no abnormal vessels in or around the hematoma. (**F**) Axial head CT image immediately after first surgery showing residual parieto-occipital hematoma, a large extradural hematoma in the left frontoparietal region (black arrowheads). (**G**) Axial CT head image after second surgery showing fresh heterogeneous area suggestive of hemorrhage in the left frontal lobe anteriorly (dashed white circle), the extradural hematoma, and midline shift has significantly resolved. Patient died few days later, however.

malformations (VMs).[12] Our case could have been BRBNS; however, cutaneous or mucosal lesions were not present, though a lesion was noted in the left lung.

True visceral hemangiomas in adults have also been reported.[13] However, the present case points toward VMs rather than true hemangiomas. A variety of VAs, isolated or syndromic exist, and the readers may refer to the latest Study of Vascular Anomalies classification for further updates.[3] A shortened list of syndromes associated with vascular tumors and malformations is provided in ►**Table 2**.

Table 2 Syndromes associated with vascular tumors and malformations

Tumors	Infantile hemangioma, PHACE syndrome
Malformations	
(a) Low-flow	Sturge–Weber syndrome, Klippel–Trenaunay syndrome, Servelle–Martorell syndrome, Proteus syndrome, Cutis marmorata telangiectatica congenital, Adams–Oliver syndrome, blue rubber bleb nevus syndrome (Bean syndrome), Maffucci syndrome, Gorham–Stout syndrome, CLAPO syndrome, CLOVES syndrome[a], Bannayan–Riley-Ruvalcaba syndrome[a]
(b) High-flow	Wyburn–Mason syndrome, Parkes–Weber syndrome, Rendu–Osler–Weber syndrome (hereditary hemorrhagic telangiectasis), Cobb syndrome, Cowden syndrome, Ehlers–Danlos syndrome, CLOVES syndrome[a], Bannayan–Riley–Ruvalcaba syndrome[a]

[a]Has both low- and high-flow lesions.

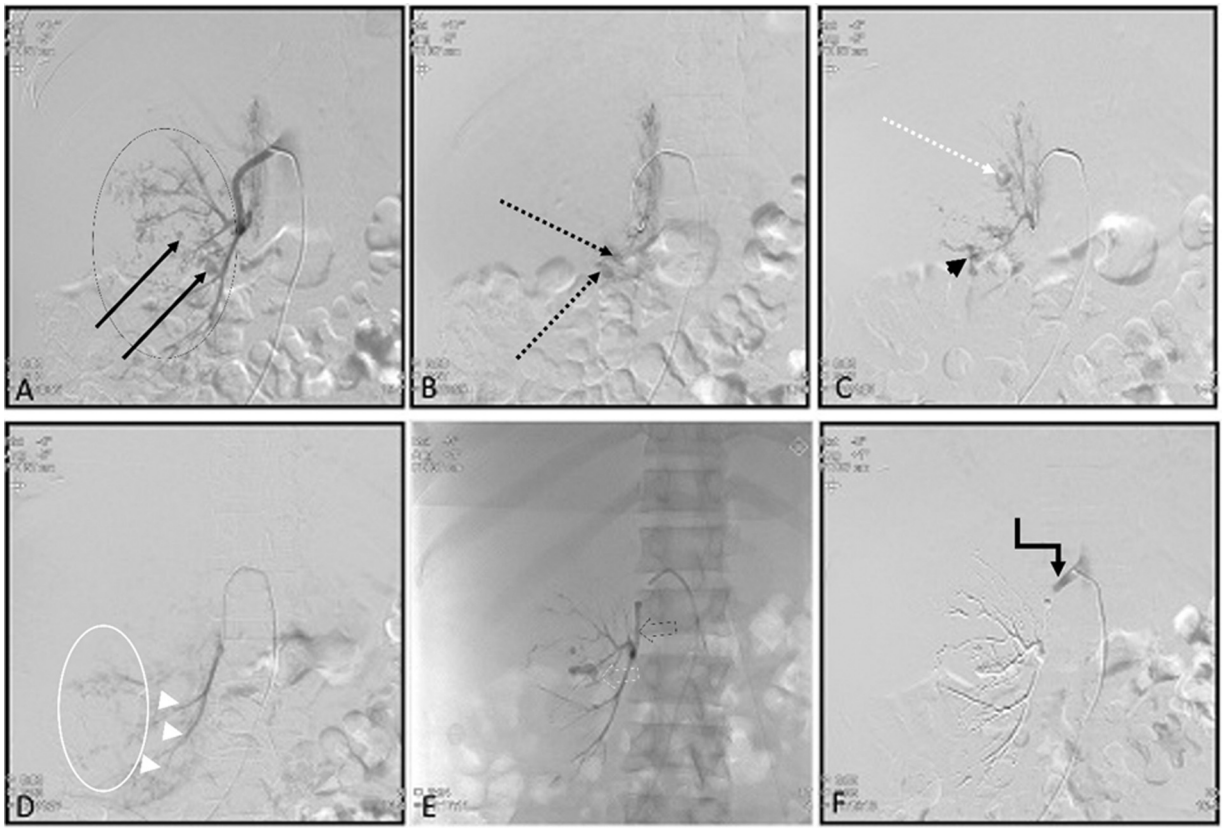

Fig. 3 Digital subtraction angiography and renal embolization image panel. (**A**) Right renal angiography image showing large mass with extensive nodularity (black oval) and aneurysms (black arrows). (**B**) Selective angiography of a posterior renal branch showing no normal parenchyma, two large aneurysms are seen inferiorly (dashed black arrows). (**C**) Selective angiography of an upper renal branch showing virtually no normal parenchyma, large irregular vascular aneurysms (white dashed arrow), and sinusoidal spaces (black arrowhead) are seen. (**D**) Selective angiography of inferior renal branch showing some straight vessels (white arrowheads), possible supplying normal renal parenchyma; however, most of the branches are supplying an area of the lesion (white ocal); at this point the right kidney was deemed non-salvageable and with discussion of the urologist, glue embolization of the whole kidney was performed using 20% nBCA-lipiodol mixture. (**E**) Fluorospot image showing glue cast of the renal artery (hollow black arrow), branches, and the abnormal vascular tree, including some of the aneurysms (hollow white arrow). (**F**) Postembolization control angiography showing patent right renal artery stump (black zig-zag arrow) with complete exclusion of the right kidney and the mass therein from circulation.

Conclusion

We present a rare and fatal case of multiorgan ruptured visceral hemangiomas with sequential ruptures, and the first report of cardiac thrombus and multiple arterial thrombotic/embolic occlusions in this setting.

Ethical Approval
The research was performed according to the Helsinki Declaration on ethical research.

Funding
None.

Conflict of Interest
None declared.

References

1 Elsayes KM, Menias CO, Dillman JR, Platt JF, Willatt JM, Heiken JP. Vascular malformation and hemangiomatosis syndromes: spectrum of imaging manifestations. AJR Am J Roentgenol 2008;190(05):1291–1299
2 Kumar S, Bhavana K, Sinha AK, et al. Image-guided percutaneous injection sclerotherapy of venous malformations. SN Compr Clin Med 2020;2:1462–1490
3 International Society for the Study of Vascular Anomalies. Accessed June 9, 2021 at: https://www.issva.org
4 Kumar S, Bhavana K, Kumar S, Kumar P. Ultrasound-guided polidocanol foam sclerotherapy for treating venous malformations. J Clin Ultrasound 2018;46(01):23–31
5 Kumar S, Bhavana K, Kumar B, Sinha AK, Kumar P. Image guided sclerotherapy of masseteric venous malformations. Ann Otol Rhinol Laryngol 2020;129(06):548–555
6 Hasan HY, Hinshaw JL, Borman EJ, Gegios A, Leverson G, Winslow ER. Assessing normal growth of hepatic hemangiomas during long-term follow-up. JAMA Surg 2014;149(12):1266–127. Erratum in: JAMA Surg. 2014;149(12):1271
7 Sethi S, Agarwal V, Chopra P. Cavernous hemangioma of the kidney: a report of two cases and review of the literature. Urol Ann 2012;4(03):187–190
8 Lee HS, Koh BH, Kim JW, et al. Radiologic findings of renal hemangioma: report of three cases. Korean J Radiol 2000;1(01): 60–63

9 Nakano TA, Zeinati C. Venous thromboembolism in pediatric vascular anomalies. Front Pediatr 2017;5:158
10 Adams DM. Special considerations in vascular anomalies: hematologic management. Clin Plast Surg 2011;38(01):153–160
11 Neto TFD, Renteria JM, Filho DB. Renal hemangioma. Int Bra J Urol. 2004;30(03):216–218
12 Chen W, Chen H, Shan G, et al. Blue rubber bleb nevus syndrome: our experience and new endoscopic management. Medicine (Baltimore) 2017;96(33):e7792
13 Tao LL, Dai Y, Yin W, Chen J. A case report of a renal anastomosing hemangioma and a literature review: an unusual variant histologically mimicking angiosarcoma. Diagn Pathol 2014;9:159

